J Appl Electrochem (2014) 44:1047–1058
DOI 10.1007/s10800-014-0703-1

RESEARCH ARTICLE

The influence of organization of LbL films containing a silsesquioxane polymer on the electrochemical response of dopamine

Cleverson Siqueira Santos · Rodolfo Thiago Ferreira · Carolina Maria Fioramonti Calixto · José Luiz Rufino · Jarem Raul Garcia · Sergio Toshio Fujiwara · Karen Wohnrath · Christiana Andrade Pessoa

Received: 1 April 2014 / Accepted: 9 June 2014 / Published online: 27 July 2014

Abstract This paper describes the construction, evaluation, and application of an electrochemical sensor for the determination of dopamine (DA) in the presence of ascorbic acid (AA) and uric acid (UA). Satisfactory results were achieved for the simultaneous determination of DA and UA, it was verified that it is possible to detect AA in the presence of DA, but high concentrations of AA interfere in detection of DA. The sensor was constructed using the layer-by-layer (LbL) technique with the modification of the surface of indium tin oxide coated glass (ITO) substrate with nanostructured films comprising a 3-*n*-propylpyridinium silsesquioxane polymer ($SiPy^{+}Cl^{-}$) and nickel(II) tetrasulfophthalocyanine (NiTsPc). Using the square wave voltammetry technique (SWV), the LbL modified electrodes produced at different pHs (pH 2 and 8) were used to determine DA in the presence UA, and the electrochemical responses of the electrodes were compared. It was observed that the electrodes with the highest concentration of monomeric species showed the highest current intensity and the lowest peak potential for the DA and UA analytes in analysis of DA and UA, individually and simultaneously, with peak potential separation of 460 mV versus Ag/AgCl. Applying SWV, a linear dynamic range of 10–99 μmol L^{-1} and 100–900 μmol L^{-1} with detection limit of 16.8 μmol L^{-1} and 58.3 μmol L^{-1} was obtained for DA and UA, respectively. The method has good selectivity and sensitivity, and it was successfully applied to the simultaneous determination of DA and UA in spiked human urine sample.

Keywords SWV · LbL · Silsesquioxane polyelectrolyte · Dopamine

C. S. Santos · R. T. Ferreira · C. M. F. Calixto · J. L. Rufino · J. R. Garcia · S. T. Fujiwara · K. Wohnrath · C. A. Pessoa (✉)
Department of Chemistry, Universidade Estadual de Ponta Grossa – UEPG, Ponta Grossa, PR 84030-000, Brazil
e-mail: christianapessoa@hotmail.com; christiana.pessoa@pq.cnpq.br

1 Introduction

Nanoscience and nanotechnology have enabled the advancement in research for the development of electrochemical sensors and biosensors. Nanoscale synthesis techniques have been widely employed to the production of functional nanoarchitectures with control of specific properties for applications in optical, electronic devices, and electrochemical sensors. An efficient way to produce nanoarchitectured materials, which can be applied as electrochemical sensors, is the deposition of multilayer films assembled on a conductive substrate surface using the layer-by-layer (LbL) technique, which is based on electrostatic interactions of positively and negatively charged polyelectrolytes. The LbL technique offers as main advantages the experimental simplicity, versatility, low cost, as well as the possibility to control film thickness and architecture at the molecular scale [1].

Several strategies have been reported in the literature using LbL techniques in order to develop electrochemical sensors. Recently, a significant number of papers addressed to the use of tetrasulfonated metallophthalocyanines [2–5] have been produced, due to their excellent physical and chemical properties and high versatility as powerful electrocatalyst that could be harnessed for the fabrication of electrochemical sensors. The phthalocyanines can present both monomeric and aggregate forms. These forms can directly influence the organization of the nanostructure

system and hence the sensitivity of the electrochemical sensor.

Santos et al. [6] observed that when nickel(II) tetrasulfophtalocyanine (NiTsPc) is assembled with poly(*0*-methoxyaniline) (POMA) in the LbL films, adsorption of the monomeric species seems to be more effective. The latter is indicated in the absorption spectrum of the 20-bilayer POMA/NiTsPc film where there is preferential growth of the band at 675 nm, characteristic of the monomeric species.

A similar effect was reported by Zucolotto et al. [7] with LbL films based on polyaniline and NiTsPc, designed as PANI/NiTsPc. This behavior was not observed for films comprising iron tetrasulfophtalocyanine (FeTsPc) and copper tetrasulfophtalocyanine (CuTsPc). However, the correlation between the prevalence of the monomeric species in the electrochemical response is not fully explored in most of the articles present in the literature.

In this paper, the propylpyridinium silsesquioxane chloride polymer (designated as $SiPy^+Cl^-$) was employed as cationic polyelectrolyte. This material is a new water-soluble polymer which presented a strong anionic exchange capacity, due to its random structure [8]. The main characteristic of this polymer is the ability of forming stable thin films on many substrate surfaces [9].

Materials based on silsesquioxane structures have been successfully applied for the electrochemical detection of DA in the presence of AA. Arguello et al. [10] reported the simultaneous determination of DA, AA, and UA at a carbon paste electrode modified with the poly-3-*n*-propyl-1-ozone-4-azabicyclo[2.2.2]octane silsesquioxane. This sensor presented potential differences of 240 and 140 mV versus saturated calomel electrode between DA and AA and between DA and UA, respectively.

Jesus et al. [9] constructed a sensor for DA using the $SiPy^+Cl^-$ along with the polyanion copper tetrasulfonated phthalocyanine (CuTsPc) immobilized on the surface of the glass substrate coated with fluorine-doped tin oxide (FTO) using the LbL technique. The electrode $(SiPy^+Cl^-/CuTsPc)_5$ determined simultaneously DA and AA with a separation of peak potential of 550 mV versus Ag/AgCl in the concentration range of 0.09–0.20 mmol L^{-1} for DA at pH 3.0. Recently, Santos et al. [11] used the $SiPy^+Cl^-$ as a nanoreactor and stabilizer for the formation of platinum nanoparticles (PtNPs), designated as Pt-$SiPy^+Cl^-$. The Pt-$SiPy^+Cl^-$ was used as a polycation in the preparation of LbL films on a glass substrate coated with fluorine-doped tin oxide (FTO) alternating with the polyanion poly(vinyl sulfonic acid) (PVS). These LbL films were tested for DA determination in the presence of AA. The simultaneous determination was performed at pH 7.0 with the following oxidation potential 900 mV versus Ag/AgCl for DA and 1,400 mV versus Ag/AgCl for AA, with a detection limit (DL) of 2.60 μmol L^{-1} and a quantification limit (QL) of 8.60 μmol L^{-1}. The films exhibited good repeatability and reproducibility.

Within this context, the main purpose of this study is to verify the influence of the LbL films organization on the electrochemical response in the simultaneous determination of DA, UA, and AA. For the construction of LbL films, the indium tin oxide coated glass (ITO) was modified with nanostructured films comprising a 3-*n*-propylpyridinium silsesquioxane polymer ($SiPy^+Cl^-$) and NiTsPc using the LbL technique. The electrode proposed in this paper presented some advantages as lower oxidation potentials for DA 300 mV versus Ag/AgCl at pH 7.0, lower number of bilayers, higher organization of the polyelectrolyte immobilized on the electrode surface, due to the higher concentration of monomers, and larger peak potential difference for the simultaneous determination of DA in presence of the interferents, in comparison to the paper presented by Santos et al. [11] and Jesus et al. [9] in which the polyelectrolyte $SiPy^+Cl^-$ was employed. Beside this, the NiTsPc organization in the LbL film was observed to considerably influence the sensitivity of the sensor for determination of dopamine in presence of AA and UA.

2 Experimental

2.1 Instrumentation and chemicals

Dopamine (DA) and NiTsPc were purchased from Aldrich Co. Ascorbic acid (AA) and uric acid (UA) were from Merck. The 3-*n*-propylpyridinium silsesquioxane polymer ($SiPy^+Cl^-$) was prepared as described in the literature [12]. All other chemical reagents were analytical grade. Solutions were prepared with doubly distilled water.

2.2 Preparation of the layer-by-layer films upon ITO substrate

Firstly, the substrates were washed using solution of hydrogen peroxide/ammonium hydroxide/water (1:1:5) at boiling temperature. Subsequently, they were dried at room temperature, immersed in isopropyl alcohol, and heated to approximately 90 °C. In the sequence, the films were immersed in chloroform and heated at 60 °C and dried in the air. Then, the surface of the ITO substrate was modified using solutions of cationic polyelectrolytes ($SiPy^+Cl^-$) and anionic (NiTsPc) with concentrations in the range of 0.50–2.00 mg L^{-1} and pH in the range of 2.0–8.0.

The multilayer deposition was performed by dip-coating technique. The substrate was alternately immersed into the $SiPy^+Cl^-$ and NiTsPc solutions for 5 min. After deposition of each layer, the substrate was rinsed with water for 10 s

to remove excess of non-adsorbed molecules and then dried in air. This procedure was repeated until the desired number of bilayers was formed. The pH of the polyelectrolyte solution and washing solution was adjusted with NaOH 0.10 mol L^{-1} to pH 8.0. The films were also deposited onto quartz, Silicon (Si), and silver (colloidal dispersion on glass) for spectroscopic characterization.

2.3 Characterization of the LbL films

The LbL films built at different pHs and concentrations were characterized using UV–Vis spectroscopy technique (VARIAN Cary-50 Bio), deposited on quartz substrate. Spectra were collected in the range from 400 to 800 nm, where the NiTsPc presents two absorption bands. The $(SiPy^{+}Cl^{-}/NiTsPc)_n$ LbL films were built with $n = 2$–22 bilayers and from every two bilayers, a spectrum was obtained.

Fourier transform infrared spectroscopy (FTIR) measurements were carried out using $(SiPy^{+}Cl^{-}/NiTsPc)_n$ LbL films, $SiPy^{+}Cl^{-}$, and NiTsPc drop-coated films deposited onto Si substrate using a SHIMADZU model 8400 FTIR and analyzed by reflectance mode in the range of 400–1,800 cm^{-1}, at 4 cm^{-1} resolution with 64 times scans.

LbL films were morphologically analyzed by atomic force microscopy (SHIMADZU SPM 9500 J3), for films with different number of bilayers (2, 10, 18, and 22) deposited on glass substrates. The films were analyzed using the non-contact mode with Silicon SPM-Sensor (Al-coating) (NANO WORD) with 4 μm thickness, 125 μm length, 30 μm width, resonance frequency of about 320 kHz and force constant 42 N/m. The software used was SPM manager version 3.03. The average roughness of the films was determined by this technique.

2.4 Electrochemical measurements

All electrochemical experiments were conducted on a micro-Autolab III Metrohm-Eco Chemie potentiostat/galvanostat electrochemical workstation using software GPES version 4.9. A conventional three-electrode electrolyte cell was used. The ITO modified with $(SiPy^{+}Cl^{-}/NiTsPc)_n$ LbL films (with an area of 0.25 cm^2) was used as working electrode (WE), the reference electrode (RE) was a Ag/AgCl electrode and a Pt wire served as counter electrode (CE).

Freshly prepared solutions of dopamine, ascorbic acid, and uric acid were used for all the experiments. The electrochemical experiments were performed in 0.10 mol L^{-1} phosphate buffer solution at pH 7.0. Cyclic voltammograms were recorded in a suitable potential range from −200 to 1,200 mV for AA and UA and for DA −200 to 600 mV. The simultaneous determination of DA, UA, and AA was carried out through square wave voltammetry (SWV) using the following conditions: $f = 10$ Hz, $a = 50$ mV, and $\Delta E_s = 1.0$ mV, in a potential range from −200 to 1,200 mV. For the analytical curve, the concentration of DA ranged from 10 to 99 μmol L^{-1} keeping the concentration of UA fixed in 470 μmol L^{-1}. For the UA analytical curve, the concentration range was from 100 to 900 μmol L^{-1}, with a fixed DA concentration of 100 μmol L^{-1}. All experiments were carried out at room temperature (i.e., 25 °C).

2.5 Procedure for human urine sample analysis

The human urine used in this study was obtained from healthy volunteers. Initially, 10.0 mL of urine sample was spiked with 100 μL of the DA and UA solution with concentration of 1.0 mmol L^{-1}. Then, 1.0 mL of this urine sample and 9.0 mL of the 0.10 mol L^{-1} phosphate buffer pH 7.0 were transferred into an electrochemical cell, in order to have 100 μmol L^{-1} of DA. Then, successive aliquots of 50.0 μL of DA 1.00 mmol L^{-1} standard solution were added into the electrochemical cell, and square wave voltammograms were recorded.

3 Results and discussion

3.1 Characterization of LbL films

Figure 1 shows the UV–Vis spectra of the polyelectrolyte solutions ($SiPy^{+}Cl^{-}$ e NiTsPc). Mathematical deconvolution was used to separate the peaks because of overlapping. For deconvolution analysis, all of the curves were generated according to the Gaussian model.

The $SiPy^{+}Cl^{-}$ spectrum did not exhibit any absorption bands in the region of 450–800 nm. The solution of NiTsPc exhibited two absorption bands, one band at 622 nm related to the aggregated form, and another at 663 nm referred to monomeric form, both of them are attributed to the $\pi \rightarrow \pi^*$ transition, from the HOMO of a_{1u} symmetry to the LUMO of e_g symmetry [13].

In the study, the process of construction of LbL films was optimized by varying the immersion time (1–5 min), pH (range of 2.0–8.0), and concentration of the polyelectrolytes solutions (0.5–2.0 mg mL^{-1}). The LbL deposition of the films was monitored using UV–Vis technique in the wavelength range of 400-800 nm. Figure 2 shows the UV–Vis spectra obtained at different pHs (Fig. 2a) and concentration of polyelectrolyte solutions (Fig. 2b).

The immersion time was fixed at 5 min when the saturation of the deposited species occurred, and the largest intensity of the absorbance bands (both monomeric and dimeric bands) was obtained (results not shown). The immersion time is set in agreement with other studies reported in the literature [9, 14].

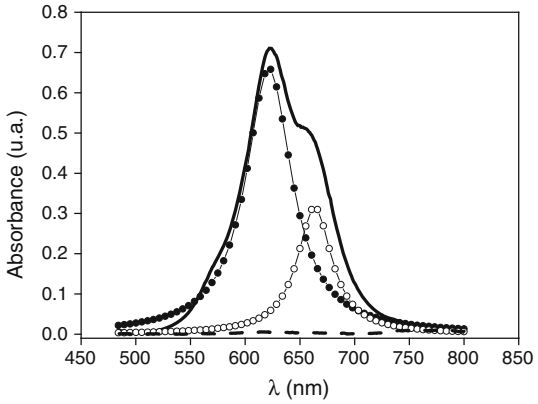

Fig. 1 UV–Vis spectra of $SiPy^+Cl^-$ (*dash line*) and NiTsPc aqueous solutions (*solid line*) with a concentration of 100 μmol L^{-1}. The *symbols* correspond to the deconvolution lines for band at 662 nm (*open circles*) and band at 622 nm (*full circles*)

In the literature, studies have shown that there is a dependence of the concentration of dimeric and monomeric species on the pH [15, 16]. In the spectrum of the NiTsPc solution, the predominant species are the aggregate ones (Fig. 1). The mean ratio between the monomeric and dimeric bands (A_{669}/A_{625}) of the species in solution of pH 8 was 0.713. However, it is interesting to mention that for the LbL films, this ratio increased gradually from pH 2 (0.725) to pH 4 (0.935) to pH 6 (1.046) to pH 8 (1.096). Although, the average ratio did not increase significantly from pH 6 to pH 8, the intensities of the bands in pH 8 increase, indicating that the concentration of immobilized species is higher (Fig. 2a). These results showed the amount of aggregates species at this pH, decrease in LbL films, compared to the solution.

In pH 8.0, it was possible to observe that the concentration of monomeric species was higher when compared with films obtained at lower pH values. This is an indication that the polyelectrolytes at pH 8 influenced the organization between the monolayers and minimize the formation of the aggregates. Wang et al. [17] found that it is possible to control the concentration of monomer and aggregate species of phthalocyanines with metallic zinc center (ZnPc) substituted with amides using the pH variation. In this study, the pH range studied ranged from 2 to 8, and it was found that in solutions with an alkaline pH, the band intensity of the monomer species is higher than the band of aggregate species.

Then, pH 8.0 was chosen for the construction of the films. Claessens et al. [18] reported that the control over the formation of molecular aggregates onto the semiconductor has been the key to achieve good efficiencies in phthalocyanines-based systems. The level of supramolecular organization of NiTsPc in LbL films with $SiPy^+Cl^-$ was evaluated based on the relative importance of dimeric and monomeric species in the films. These authors concluded that high concentration of monomeric species is correlated with an enhanced organization of the immobilized species on the electrode surface.

In Fig. 2b, using different concentrations of the polyelectrolyte solutions, it can be observed that as their concentration is increased, the absorbance of both monomeric and dimeric species is also increased. Therefore, the concentration of 2.0 mg mL^{-1} was chosen for the construction of the films. For concentrations above 2.0 mg mL^{-1} of NiTsPc, the aggregation of NiTsPc molecules is higher, which compromises the organization of the films. The films $(SiPy^+Cl^-/NiTsPc)_n$ obtained in the optimized conditions (pH 8.0 and immersion time of 5 min) with different number of bilayers were also characterized using the technique of UV–Vis, as shown in Fig. 3.

The absorbance of the monomeric band (669 nm) as the band referred to the aggregate form (625 nm) linearly increased with the number of bilayers, with the following correlation coefficients 0.998 and 0.996, respectively. Comparing the spectra of the NiTsPc solution with the LbL films, displacements of the Q bands for the $SiPy^+Cl^-$/NiTsPc were observed. For NiTsPc in solution, the Q bands were observed at 622 and 662 nm. However, for the LbL

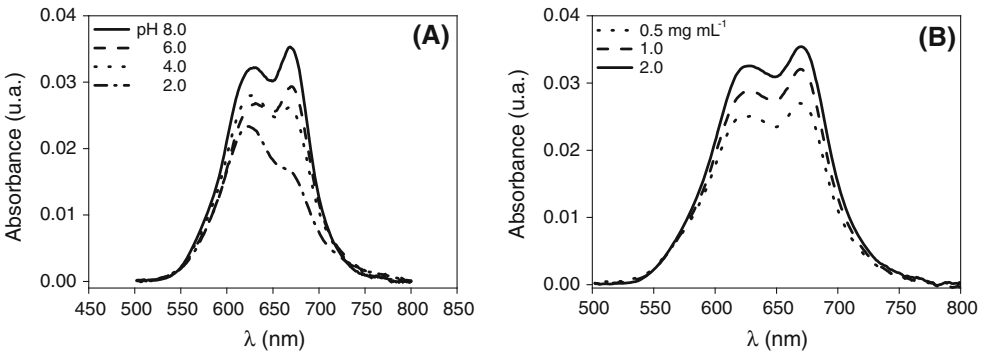

Fig. 2 UV–Vis absorption spectra of LbL film $(SiPy^+Cl^-/NiTsPc)_2$. **a** Prepared at different pHs, with fixed concentration of the polyelectrolytes solutions of 2.0 mg mL^{-1}. **b** In different concentrations of the polyelectrolyte at pH = 8.0, in both studies, the immersion time was 5 min

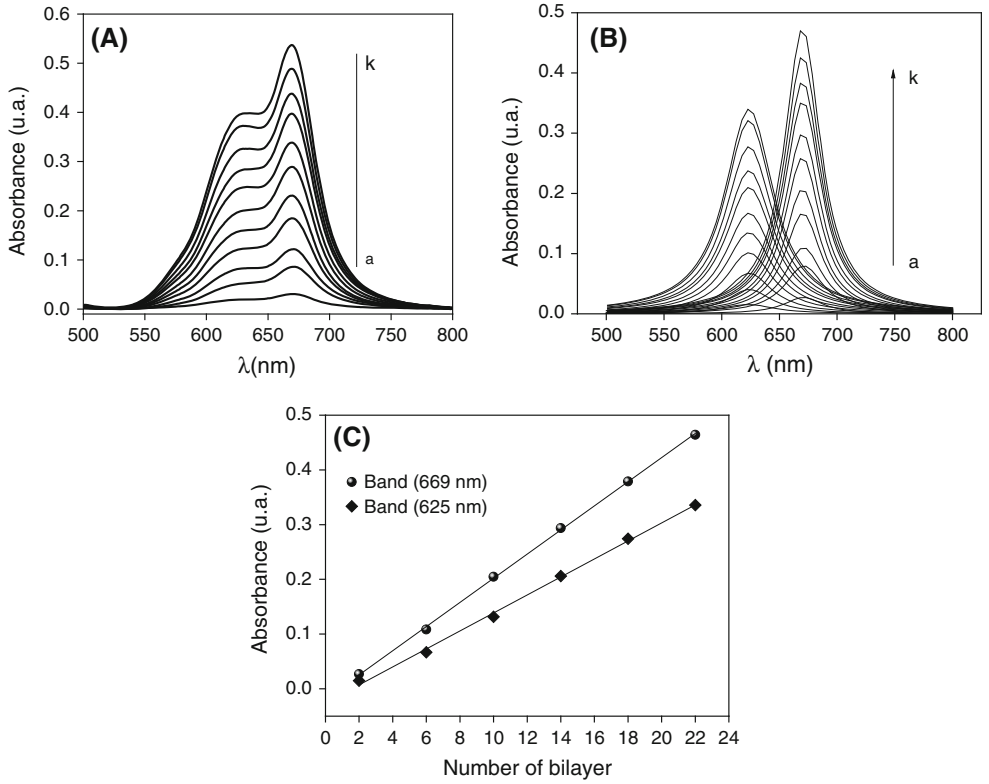

Fig. 3 **a** UV–Vis spectra for $(SiPy^{+}Cl^{-}/NiTsPc)_n$ LbL films with different number of bilayers (n = 2(a)–22(k)). **b** Deconvolution of UV–Vis spectra of the LbL films with different number of bilayers (2(a)–22(k)). **c** Relationship between the absorbance of Q-band at 625 and 669 nm as a function of the number of bilayers

films, it was observed that these bands were shifted to longer wavelengths at 625 and 669 nm. These changes are attributed to the conformation adopted by the molecules within the film or by molecular interactions between the polyelectrolyte materials [9, 19].

Moreover, it was observed that for all bilayers deposition, the spectra profile revealed that the band at 669 nm is more intense compared to dimeric band, indicating that NiTsPc molecules when immobilized at LbL films preferentially adopt the monomeric form.

To confirm the interaction between polyelectrolytes $SiPy^{+}Cl^{-}$ and NiTsPc in the formation of LbL films, these films were characterized by FTIR spectroscopy. Figure 4 shows the FTIR spectra of $SiPy^{+}Cl^{-}$, NiTsPc, and LbL film $(SiPy^{+}Cl^{-}/NiTsPc)_{35}$.

The FTIR spectrum of neat $SiPy^{+}Cl^{-}$ showed a strong and broad band at 1,090 cm^{-1}, which is assigned to the asymmetric stretching and deformation of the Si–O–Si group, besides vibrational bands at 1,487 and 1,632 cm^{-1} characteristic of the pyridinium ring and at 774 and 460 cm^{-1} attributed to the symmetric stretching group Si–O–Si [20]. The spectrum of the NiTsPc cast film presented two bands related to SO_3^{-} stretching band region at 1,033 cm^{-1} and the other at 1,190 cm^{-1}. These same bands were observed in the spectra of the LbL films but

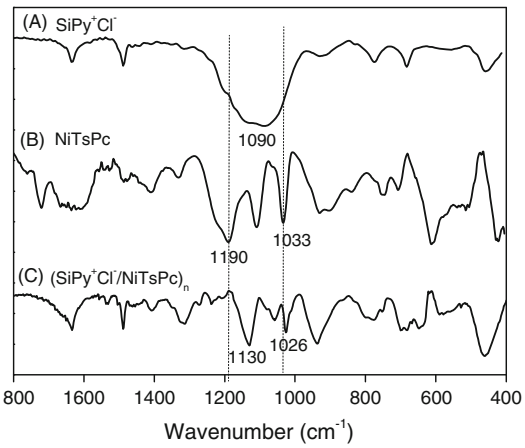

Fig. 4 FTIR spectra for films of *a* drop-coated $SiPy^{+}Cl^{-}$, *b* drop-coated NiTsPc, and *c* $(SiPy^{+}Cl^{-}/NiTsPc)_{35}$ LbL film in transmission mode

displaced to lower wavelengths of 1,026 and 1,130 cm^{-1}, respectively. Such shifts of the bands to lower wavelengths can be attributed to the electrostatic interactions between the sulfonic acid groups (SO_3^{-}) present in the molecule of NiTsPc and the pyridinium ring $SiPy^{+}Cl^{-}$ and also the hydrogen bonds [9, 19].

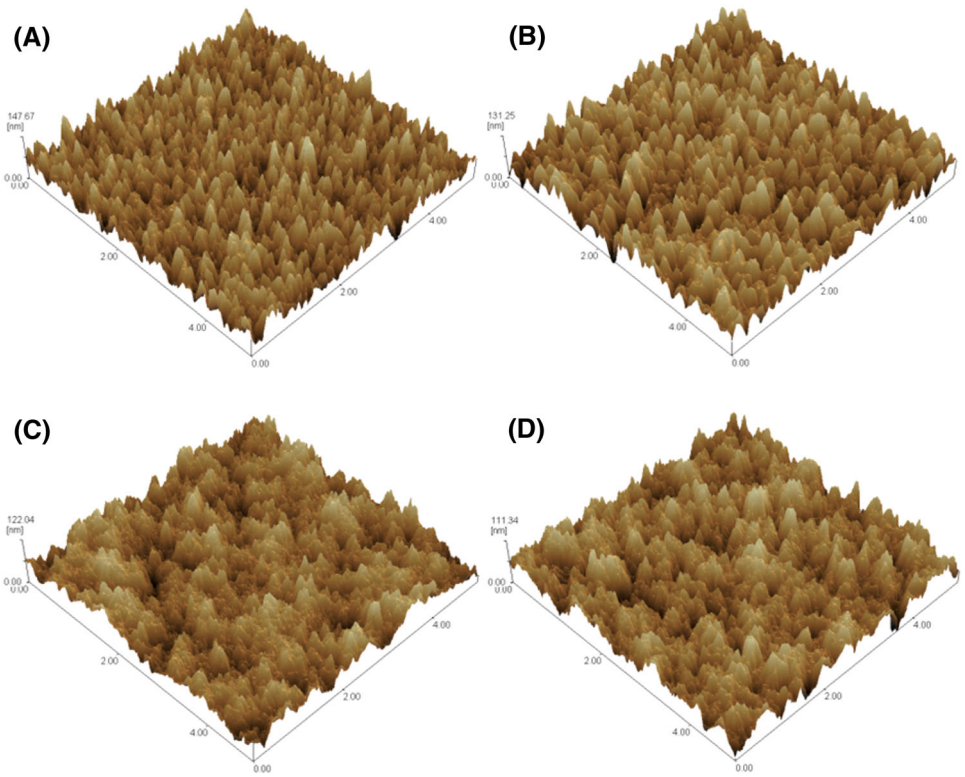

Fig. 5 3D atomic force microscopy images (5.0 × 5.0 μm) of the modified electrodes with LbL films. **a** $(SiPy^{+}Cl^{-}/NiTsPc)_2$, **b** $(SiPy^{+}Cl^{-}/NiTsPc)_{10}$, **c** $(SiPy^{+}Cl^{-}/NiTsPc)_{18}$, and **d** $(SiPy^{+}Cl^{-}/NiTsPc)_{22}$

Table 1 Average roughness of the films $(SiPy^{+}Cl^{-}/NiTsPc)_n$

Film	Number of bilayers	Average roughness (nm)	I^{a}_{pa} (μA)
$(SiPy^{+}Cl^{-}/NiTsPc)_n$	2	25.0	42.70
	10	20.4	2.72
	18	18.7	1.54
	22	16.4	1.03

[a] These current values are due to the DA oxidation at $(SiPy^{+}Cl^{-}/NiTsPc)_n$, ($n$ = number of bilayers)

AFM was also used to verify the roughness of the films. The morphological characterization of the films $(SiPy^{+}Cl^{-}/NiTsPc)_n$ (n = 2, 10, 18, and 22 bilayers) is shown in Fig. 5.

AFM characterization revealed that the average roughness of the films decreased with the increased number of bilayers. This decrease in the roughness is probably associated with the interpenetration between the monolayers [21–23]. The decrease of roughness from 2-bilayer film to 22-bilayer can be explained by the fact that possibly, during the deposition of the first bilayers, molecules are deposited randomly until covering the whole substrate, thus yielding low roughness. In this stage, adsorption is highly favored because of the attractive forces between the molecules in solution and the substrate [9, 23].

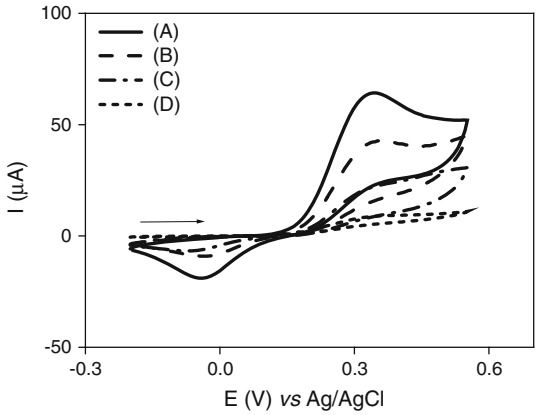

Fig. 6 Cyclic voltamogramms for **a** $(NiTsPc)_2$, **b** $(SiPy^{+}Cl^{-}/NiTsPc)_2$, **c** ITO substrate, and **d** $(SiPy^{+}Cl^{-})_2$ in the presence of DA 1.00 mmol L^{-1} in PBS, pH 7.0, v = 50 mV s^{-1}

The results of the morphological characterization were compared with the voltammetric studies, and the correlation is shown in Table 1.

It is verified that with increasing the number of bilayers, a decrease in the average roughness and also in the current intensity was observed, which can be attributed to the disorganization of the species on the electrode surface due to the increased bilayers, hindering the electron transfer process. From the results presented in Table 1, the electrode $(SiPy^{+}Cl^{-}/NiTsPc)_2$ was chosen because it presented the highest anodic peak current value for DA.

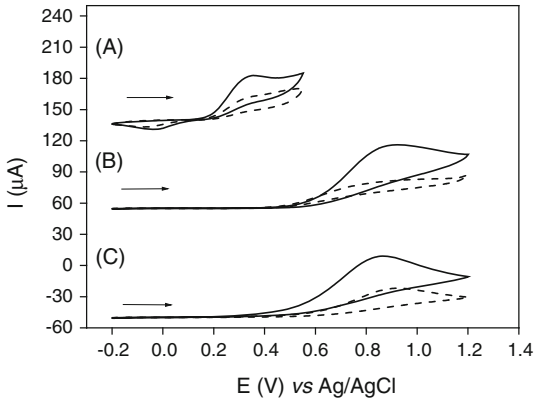

Fig. 7 Cyclic voltammograms for *a* DA 1.00 mmol L^{-1}, *b* UA 1.00 mmol L^{-1}, and *c* AA 1.00 mmol L^{-1} at $(SiPy^+Cl^-/NiTsPc)_2$. (*solid line*) and ITO (*dashed line*) Supporting electrolyte: 0.10 mol L^{-1} PBS (pH 7.0), $v = 50$ mV s^{-1}

3.2 Voltammetric behavior of DA, AA, and UA

LbL films were built with different architectures in order to investigate their electrochemical responses. Figure 6 shows the cyclic voltamogramms for $(NiTsPc)_2$, $(SiPy^+Cl^-)_2$, $(SiPy^+Cl^-/NiTsPc)_2$, and ITO substrate in presence of DA 1.0 mmol L^{-1} in phosphate buffer solutions (PBS).

The two-layer films of $(NiTsPc)_2$ showed the highest intensity of anodic peak current for DA, due to the electrocatalytic properties of the metallated phthalocyanines. However, the films containing only NiTsPc are unstable, losing material to the solution when successive electrochemical measurements were carried out, with consequent decrease in the current. The instability of the films $(NiTsPc)_2$ ($I_{pa} = 63.8$ μA) is likely to occur due to charge repulsion, because the molecule has a negative charge NiTsPc as well as the surface of the ITO substrate. Films containing only $SiPy^+Cl^-$ showed the lowest peak currents ($I_{pa} = 8.8$ μA), because the polyelectrolyte molecules were not electroactive. For the LbL films $(SiPy^+Cl^-/NiTsPc)_2$, a higher anodic current was obtained ($I_{pa} = 42.7$ μA). Despite the fact that the polyelectrolyte $SiPy^+Cl^-$ species are not electroactive, it is essential to the construction of the LbL film, in order to maintain the stability of the NiTsPc in the LbL film.

In order to study the simultaneous determination of dopamine, uric acid, and ascorbic acid in aqueous solution using the $(SiPy^+Cl^-/NiTsPc)_2$ film, the response of the electrode was verified separately by cyclic voltammetry with 1.00 mmol L^{-1} of each of these species in PBS pH 7.0. The voltammograms are presented in Fig. 7.

A single well-defined and irreversible peak was observed at 350 mV for DA, 860 mV for AA, and 900 mV for UA versus Ag/AgCl. These E_p values are the result of the electrocatalytic oxidation of the DA, AA, and UA at the $(SiPy^+Cl^-/NiTsPc)_2$ LbL film modified electrode. The

Table 2 Comparison of the electrochemical behavior of $(SiPy^+Cl^-/NiTsPc)_2$ with the unmodified electrode

Electrode	I_{pa} (μA) for DA	I_{pa} (μA) for UA	I_{pa} (μA) for AA
$(SiPy^+Cl^-/NiTsPc)_2$	42.0	58.0	61.0
ITO	7.3	14.6	7.4

Table 2 exhibits the comparing of the results obtained from the LbL films and the ITO substrate.

It can be observed that although the $(SiPy^+Cl^-/NiTsPc)_2$ and ITO electrodes oxidized DA, AA, and UA at similar potentials (340, 850, and 920 mV, respectively), different current intensities were obtained. The voltammograms obtained using LbL films showed higher current values for DA, AA, and UA when compared to those obtained with the unmodified ITO. However, it can be observed that the oxidation potential for DA is smaller, and oxidation potential of AA and UA is shifted to more positive values in relation to the potential obtained by conventional electrodes as glassy carbon electrodes (DA = 380 mV, AA = 200 mV, and UA = 500 mV versus Ag/AgCl) [24]. This fact may be explained considering the $pK_a = 4.17$ for AA and $pK_a = 5.75$ for UA, which indicates that at pH 7.0, both species are in the anionic form of the ascorbate (AA^-) and urate (UA^-) [25, 26]. As the outside surface of the film $(SiPy^+Cl^-/NiTsPc)_2$ has $NiTsPc^{4-}$ anion exposed, it probably repels the anionic species AA^- and UA^- increasing the oxidation potential for these species. Similar behavior was observed by Wang et al. [27] for the amperometric determination of cationic neurotransmitters through a glassy carbon electrode modified with Nafion®. Furthermore, Manjunatha et al. [26] applied a graphite electrode modified with sulfonated polystyrene and carbon nanotubes for the simultaneous determination of ascorbic acid, dopamine, and uric acid. These authors observed that dopamine ($pK_a = 8.92$) at pH 7.0 exists in cationic form and is attracted by films which are modified by the anionic surface carbon. In contrast, the anionic species AA and UA are repelled by the negatively charged surface of the electrodes.

3.3 Square wave voltammetric studies

Using the square wave voltammetry, the LbL electrodes obtained at different pHs of the polyelectrolyte solutions (pH 2.0 and 8.0) were used to determine DA in the presence of UA, and the electrochemical responses of the electrodes were compared (Fig. 8).

From the pH study, it was observed that the electrodes built with the polyelectrolyte solutions at pH 8.0 (which presents the most intense band related to the monomeric

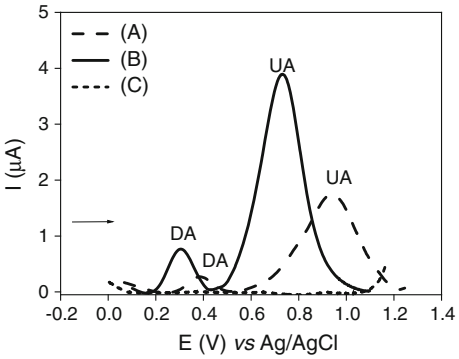

Fig. 8 Square wave voltammograms for DA 1.00 mmol L^{-1} in the presence of UA 1.00 mmol L^{-1} obtained of the $(SiPy^{+}Cl^{-}/NiTsPc)_2$ constructed using of the polyelectrolytes solutions at *a* pH 2.0 and *b* pH 8.0 *c* absence of the electroactive species, in PBS 0.10 mol L^{-1}, pH 7.0

form, as can be seen in Fig. 2a) were those with the highest intensity peak current and lower oxidation peak potential when compared with the films built at pH 2.0, in the simultaneous detection of DA and UA. These results were an indicative that the organization of the polyelectrolyte molecules immobilized on the surface of the substrate influences the electrode sensitivity in the detection of DA and UA. One explanation for this behavior is that the aggregation of the molecules on NiTsPc films decreases the number of electroactive sites thus decreasing the electroactivity of the sensor [28]. Therefore, the electrode constructed with solutions of polyelectrolytes at pH 8.0 with two bilayers was chosen for the further measures. Figure 9 shows the results of simultaneous determination of DA in the presence of UA and AA.

The electrode proved satisfactory for the simultaneous determination of DA and UA because voltammetric oxidation peaks of these two species are separated into two well-defined oxidation peaks at potentials around 320 and 790 mV, respectively. The separation between the two peak potentials is large enough ($\Delta E_p \sim 470$ mV).

Also, the SWV peaks of DA and AA are separated into two well-defined oxidation peaks at potentials around 300 and 760 mV, respectively. With peak potential difference of 460 mV, which also enable the determination of DA in the presence of AA (Fig. 9b). Nevertheless, it is not possible to determine UA and AA at the approximately same sample potential (760 mV). These results show that the electrode is able to determine DA in the presence of UA and AA; however, it is not able to discriminate UA from AA.

The SWV voltammograms of Fig. 9a, b, c were obtained using the same DA concentration. Comparing the oxidation peak currents of DA presented in voltammograms, it was observed that the current intensity for DA varies with high concentrations of AA (Fig. 9c). One explanation for this behavior is that the oxidation product of DA (dopamineequinone) can react with AA in solution, reducing it again to the dopamine, forming a cycle [29, 30]. For this reason, the

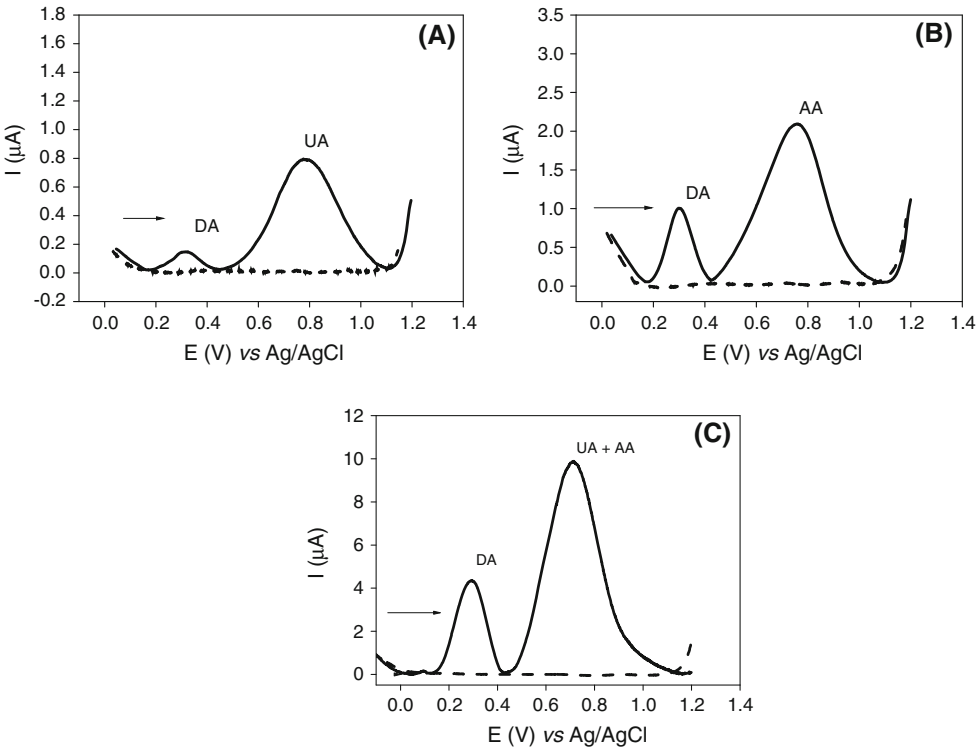

Fig. 9 **a** Square wave voltammograms for DA 10.0 μmol L^{-1} in the presence of UA 470 μmol L^{-1} (*solid line*), **b** for DA 10.0 μmol L^{-1} in the presence of AA 470 μmol L^{-1} (*solid line*), **c** for DA 10.0 μmol L^{-1} in the presence of UA 470 μmol L^{-1} and AA 470 μmol L^{-1} (*solid line*), obtained on $(SiPy^{+}Cl^{-}/NiTsPc)_2$, and absence of electroactive species (*dash line*), in PBS 0.10 mol L^{-1}, pH 7.0

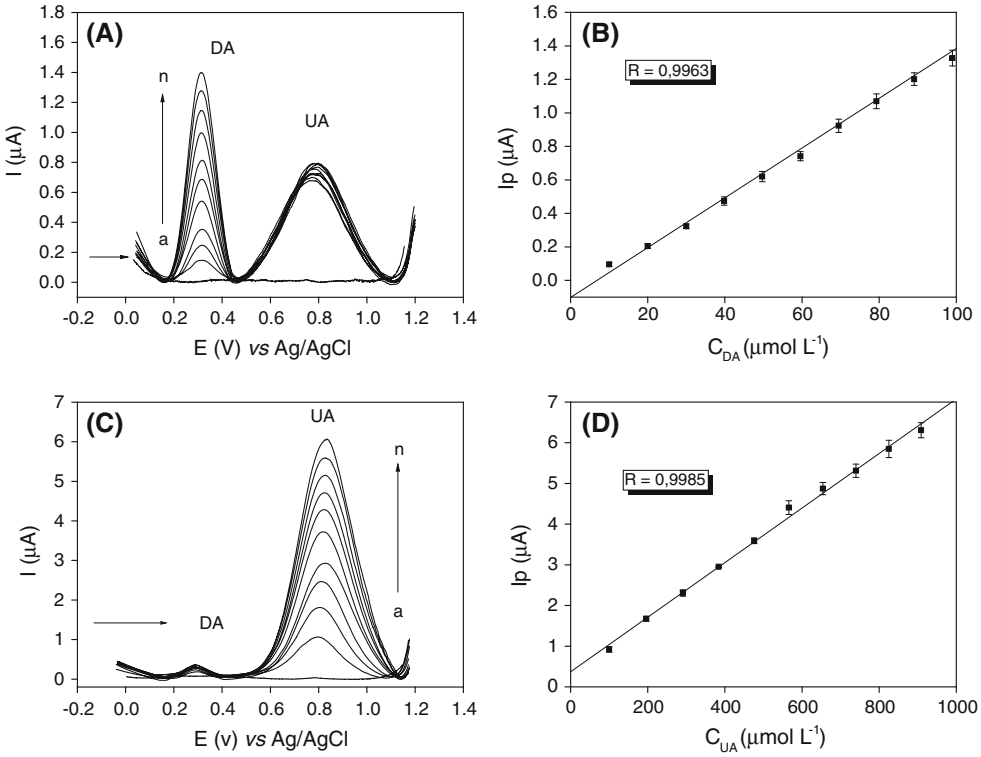

Fig. 10 SWVs. **a** solutions containing 470 μmol L^{-1} of UA, and (a) without DA, (b–n) with DA of 10.0–99.0 μmol L^{-1}, **b** analytical curve of DA, **c** SWVs of solutions containing 100 μmol L^{-1} of DA, (*a*) without UA, (*b–n*) with UA of 100–900 μmol L^{-1}, **d** Analytical curve for UA. Supporting electrolyte: 0.10 mol L^{-1} PBS (pH 7.0)

Table 3 Analytic parameters for DA and UA, at $(SiPy^{+}Cl^{-}/NiTsPc)_2$ electrode

Analytes	Linear Range μmol L^{-1}	Sensitivity/A mol L^{-1}	DL μmol L^{-1}	QL μmol L^{-1}
DA	10.0–99.0	0.014	16.8	56.0
UA	100–900	0.007	58.3	194.0

peak current intensity may not be related to the actual dopamine concentration. Therefore, further experiments were carried out using DA in presence of UA.

3.4 Analytical performance

The analytical curves were obtained, using PBS solution 0.10 mol L^{-1}, at pH 7.0. Figure 10a shows the SWV curves of DA at different concentrations in the presence of UA with a fixed concentration of 470 μmol L^{-1}, and Fig. 10b shows the SWV curves of UA at various concentrations in the presence of DA with fixed concentration of 100 μmol L^{-1}.

We found that it is possible to determine DA in the presence of UA as well as UA in presence of DA, because the electrode was sensitive and selective in the range studied. The analytical parameters for both DA and AA determination are presented in the Table 3.

It can be found that the SWV peak height is linearly related to the DA and UA concentration intervals: 10.0–99.0 and 100–900 μmol L^{-1}, respectively. Repeatability for the $(SiPy^{+}Cl^{-}/NiTsPc)_2$ electrode was measured in three different experiments ($n = 3$). The limits of detection and quantification were 16.8 μmol L^{-1} and 56.0 μmol L^{-1} for DA and 58.3 μmol L^{-1} and 194.0 μmol L^{-1} for UA. The LD and LQ were determined as $3\sigma/b$ ratio and $10\sigma/b$, respectively, where σ is the standard derivation of the mean value for 10 voltammograms of the blank, and b is the angular coefficient of straight line, determined according to the IUPAC recommendations [31].

In Table 4, there is a comparison between the analytical parameters displayed by these electrodes with other studies reported in the literature.

Comparing the results in Table 4, it can be verified that this modified electrode $(SiPy^{+}Cl^{-}/NiTsPc)_2$ can be assigned to the efficiency of the transfer of electrons between the analytes DA and UA, the sensor showed a well-defined anodic peak for the DA oxidation, distinct from of the peak of the UA oxidation with a large peak potential difference of 470 mV. The detection limits are similar to those reported in this paper, but the separation of potential peak between species is higher [9, 11, 32, 36]. This is an advantage, because it enables the simultaneous analysis of these species.

3.5 Human urine sample analysis

In order to a sensitive and selective methods for the quantification of DA and UA, $(SiPy^{+}Cl^{-}/NiTsPc)_2$ LbL

Table 4 Comparison between the proposed sensor performance for simultaneous detection of DA and UA with others sensors based on different matrices

Electrode	Technique	LD (μM)		Linear range (μM)		ΔE_p (mV)[l]	References
		DA	UA	DA	UA		
GCE[a]/La-MWCNTs[b]	CA[c]	0.013	0.015	0.04–890	0.04–810	150	[6]
GCE/AuNP[d]/PANI[e]	DPV[f]	3.0	20.0	7.0–148	29.0–441	110	[32]
PCF[g]	DPV	0.04	0.03	0.1–9.8	0.1–9.8	154	[33]
GCE/Chit[h]/Graph[i]	DPV	1.0	2.0	1.0–24.0	2.0–45.0	90	[34]
PGE[j]-DA[k]	DPV	0.1	1.4	1.0–2.0	2.5–3.0	138	[35]
ITO/SiPy$^+$Cl$^-$/NiTsPc	SWV	2.3	5.2	10.0–99.0	100–900	470	This work

[a] GCE_Glassy carbon electrode

[b] La-MWCNTs_Lanthanum–multiwalled carbon nanotube nanocomposites

[c] CA_Chronoamperometry

[d] AuNP_Gold nanoparticles

[e] PANI_Polyaniline

[f] DPV_Differential pulse voltammetry

[g] PCF_Pyrolytic carbon film

[h] Chit_Chitosan

[i] Graph_Graphene

[j] PGE_Pyrolytic graphite

[k] DA_Dopamine

[l] Δ*E*p_oxidation peak separation between DA and UA

electrode was used in the analysis of the human urine sample which was spiked with DA 100 μmol L^{-1}. This spiked level was chosen considering the linear range of the proposed procedure.

For the voltammetric determination of the amount of DA and UA present in urine sample, the standard addition method was used. The results obtained are shown in Table 5.

Each composite was subjected to three independent measurements. The average recovery was 100.3 %, suggesting that this sensor had good selectivity toward simultaneous determination of DA and UA in the real sample analysis.

Table 5 Measurements results for DA in the presence of UA in human urine samples

Real sample	DA added (μmol L^{-1})	DA found[a] (μmol L^{-1}) ± SD	Recovery (%)
1	100	103.0 + 1.65	103.0
2	150	149.0 + 2.70	99.3
3	200	197.0 + 1.46	98.5

[a] Average of the tree determinations

4 Conclusion

In this paper it was verified that the films built in basic pH (pH 8.0) presented a higher concentration of monomers in relation to aggregates, which influences the electrochemical response of the sensor because the LbL films built at pH 8.0 presented more sensitive for the simultaneous detection of DA and UA.

The results demonstrated the modified sensor (SiPy$^+$Cl$^-$/NiTsPc)$_2$ as an attractive alternative for the simultaneous determination of DA and UA with larger peak potential difference of 470 mV.

The electrode developed has advantages over other similar, as potential peak separation, number of bilayers, and the high organization of polyelectrolyte immobilized on the electrode surface.

The good selectivity, low detection limit, rapid response, easy to prepare, and low-coast of fabrication make this modified electrode suitable for simultaneous analysis of DA and UA in human urine samples.

In the future, the base-formed (SiPy$^+$Cl$^-$/NiTsPc)$_2$ can be used to anchor biomolecules, like in the construction of biosensor.

Acknowledgments We would like to thank Conselho Nacional de Desenvolvimento Científico e Tecnológico, Coordenação de Aperfeiçoamento de Pessoal de Nível Superior and Fundação ARAUCARIA (Brazil), for financial support.

References

1. Caseli L, Santos DS, Foschini MD, Gonçalves D, Oliveira ON Jr (2006) The effect of the layer structure on the activity of immobilized enzymes in ultrathin films. J Colloid Interface Sci 303:326–331. doi:10.1016/j.jcis.2006.07.013
2. Alencar WS, Crespilho FN, Santos MRMC, Zucolotto V, Oliveira ON, Silva WC (2007) Influence of film architecture on the charge-transfer reactions of metallophthalocyanine layer-by-layer films. J Phys Chem C 111:12817–12821. doi:10.1021/jp070695r
3. Mahabul S, Rao VK, Gupta M, Pandey P (2012) Layer-by-layer self-assembling copper tetrasulfonated phthalocyanine on carbon nanotube modified glassy carbon electrode for electro-oxidation of 2-mercaptoethanol. Thin Solid Films 526:256–260. doi:10.1016/j.tsf.2012.10.121
4. Zhang YQ, Fan YJ, Cheng L, Fan LL, Wang ZY, Zhong JP, Wu LN, Shen XC, Shi ZJ (2013) A novel glucose biosensor based on the immobilization of glucose oxidase on layer-by-layer assembly film of copper phthalocyanine functionalized grapheme. Electrochim Acta 104:178–184. doi:10.1016/j.electacta.2013.04.099
5. Zampa MF, Araujo IMS, Junior JRS, Zucolotto V, Leite JRSA, Eiras C (2012) Multilayer films electrodes consisted of cashew gum and polyaniline assembled by the layer-by-layer technique: electrochemical characterization and its use for dopamine determination. Int J Anal Chem 2012:1–7. doi:10.1155/2012/923208
6. Santos AC, Zucolotto V, Constantino CJL, Cunha HN, Santos JR, Eiras C (2007) Electroactive LbL films of metallic phthalocyanines and poly(0-methoxyaniline) for sensing. J Solid State Electrochem 11:1505–1510. doi:10.1007/s10008-007-0338-9
7. Zucolotto V, Ferreira M, Cordeiro MR, Constantino CJL, Moreira WC, Oliveira ON Jr (2006) Nanoscale processing of polyaniline and phthalocyanines for sensing applications. Sens Actuators B 113:809–815. doi:10.1016/j.snb.2005.03.114
8. Benvenutti EV, Moro CC, Costa TMH, Gallas MR (2009) Materiais híbridos à base de sílica obtidos pelo método sol-gel. Quim Nova 7:1926–1933. doi:10.1590/S0100-40422009000700039
9. Jesus CG, Santos V, Canestraro CD, Zucolotto V, Fujiwara ST, Gushikem Y, Wohnrath K, Pessoa CA (2011) Silsesquioxane as a new building block material for modified electrodes fabrication and application as neurotransmitters sensors. J Nanosci Nanotechnol 11:1–10. doi:10.1166/jnn.2011.3733
10. Arguello J, Magosso HA, Canevari TC, Landers R, Gushikem Y (2011) Activity of SiDbCl in the electrooxidation of ascorbic acid, dopamine, and uric acid. Electroanalysis 23:334–338. doi:10.1002/elan.201000390
11. Santos V, Jesus CG, Santos M, Canestraro CD, Zucolotto V, Fujiwara ST, Garcia JR, Pessoa CA, Wohnrath K (2012) Platinum nanoparticles incorporated in silsesquioxane for use in LbL films for the simultaneous detection of dopamine and ascorbic acid. J Nanopart Res 14:1081. doi:10.1007/s11051-012-1081-4
12. Alfaya RVS, Gusshikem Y, Alfaya AAS (2001) Patent BR9803053-A, 20
13. Leznoff CC, Lever ABP (1989) Phthalocyanines-properties and applications, 1st edn. Wiley
14. Eiras C, Zampa MF, Brito ACF, Kitagawa IL, Constantino CJL, Oliveira ON Jr, Cunha HN, Zucolotto V, Santos JR Jr (2007) Natural gum-assisted phthalocyanine immobilization in electroactive nanocomposites: physicochemical characterization and sensing applications. Biomacromolecules 8:3408–3413. doi:10.1021/bm700528u
15. Ostler RB, Scully AD, Taylor AG, Gould IR, Smith TA, Waite A, Phillips D (2000) The effect of pH on the photophysics and photochemistry of disulphonated aluminum phthalocyanine. Photochem Photobiol 71:397–404. doi:10.1562/00318655(2000)0710397teopot2.0.co2
16. Constantino CJL, Alessio P, Mendez MLR, Saez JA (2010) Iron phthalocyanine in non-aqueous medium forming layer-by-layer films: growth mechanism, molecular architecture and applications. Phys Chem Chem Phys 12:3972–3983. doi:10.1039/B922242C
17. Wang A, Chen X, Zhang L, Zhang G, Zhou L, Lu S, Zhou J, Wei S (2014) Effects of pH on aggregation and photodynamic activities of cationic zinc phthalocyanines substituted with amides. J Photochem Photobiol A 288:1–12. doi:10.1016/j.jphotochem.2014.05.003
18. Claesses CG, Hahn U, Torres T (2008) Phthalocyanines: from outstanding electronic properties to emerging applications. Chem Rec 8:75–97. doi:10.1002/tcr.20139
19. Alencar WS, Crespilho FN, Martins MVA, Zucolotto V, Oliveira ON Jr (2009) Synergistic interaction between gold nanoparticles and nickel phthalocyanine in layer-by-layer (LbL) films: evidence of constitutional dynamic chemistry (CDC). Phys Chem Chem Phys 11:5086–5091. doi:10.1039/b821915j
20. Canevari TC, Arguello J, Francisco MSP, Gushikem Y (2007) Cobalt phthalocyanine prepared in situ on a sol–gel derived SiO_2/SnO_2 mixed oxide: application in electrocatalytic oxidation of oxalic acid. J Electroanal Chem 609:61–67. doi:10.1016/j.jelechem.2007.06.006
21. Sun J, Li Y, Wang X (2012) Layer-by-layer assembly for rapid fabrication of thick polymeric films. Chem Soc Rev 41:5998–6009. doi:10.1002/aic.12769
22. Liu G, Zhao J, Sun Q, Zhang G (2008) Role of chain interpenetration in layer-by-layer deposition of polyelectrolytes. J Phys Chem B 112:3333–3338. doi:10.1021/jp710600f
23. Batys P, Weronski P (2012) Modeling of LbL multilayers with controlled thickness, roughness, and specific surface area. J Chem Phys 137:214701–214706. doi:10.1063/1.4769390
24. Kalimuthu P, John SA (2009) Electropolymerized film of functionalized thiadiazole on glassy carbon electrode for the simultaneous determination of ascorbic acid, dopamine and uric acid. Bioelectrochemistry 77:13–18. doi:10.1016/j.bioelechem.2009.04.010
25. Prakash S, Chkrabarty T, Rajesh MA, Shahi VK (2012) Investigation of polyelectrolyte for electrochemical detection of uric acid in presence of ascorbic acid. Measurement 45:500–506. doi:10.1016/j.measurement.2011.10.022
26. Manjunatha R, Suresh GS, Melo JS, Souza SF, Venkatesha TV (2010) Simultaneous determination of ascorbic acid, dopamine and uric acid using polystyrene sulfonate wrapped multiwalled carbon nanotubes bound to graphite electrode through layer-by-layer technique. Sens Actuators B 145:643–650. doi:10.1016/j.snb.2010.01.011
27. Wang J, Tuzhi P, Golden T (1987) Amperometric detection of cationic neurotransmitters at nafion-coated glassy carbon electrodes in flow streams. Anal Chim Acta 194:129–138. doi:10.1016/S0003-2670(00)84766-2
28. Oliveira ON Jr, Siqueira JR Jr, Gasparotto LHS, Crespilho FN, Carvalho AJF, Zucolotto V (2006) Physicochemical properties and sensing ability of metallophthalocyanines/chitosan nanocomposites. J Phys Chem B 110:22690–22694. doi:10.1021/jp0649089
29. Shervedani RK, Bagherzadeh M, Mozaffari SA (2006) Determination of dopamine in the presence of high concentration of ascorbic acid by using gold cysteamine self-assembled monolayers as a nanosensor. Sens Actuators B 115:614–621. doi:10.1016/j.snb.2005.10.027
30. He H, Ali SR, Parajuli RR, Ma Y, Balogun Y (2007) Interference of ascorbic acid in the sensitive detection of dopamine by a non-oxidative sensing approach. J Phys Chem B 111:12275–12281. doi:10.1021/jp073705x

31. Analytical Methods Committee (1987) Recommendations for the definition, estimation and use of the detection limit. Analyst 112:199–204. doi:10.1039/AN9871200199
32. Stoyanova A, Ivanov S, Tsakova V, Bund A (2011) Au nanoparticle–polyaniline nanocomposite layers obtained through layer-by-layer adsorption for the simultaneous determination of dopamine and uric acid. Electrochim Acta 56:3693–3699. doi:10.1016/j.electacta.2010.09.054
33. Hadi M, Rouhollhi A (2012) Simultaneous electrochemical sensing of ascorbic acid, dopamine and uric acid at anodized nanocrystalline graphite-like pyrolytic carbon film electrode. Anal Chim Acta 721:55–60. doi:10.1016/j.aca.2012.01.051
34. Han D, Han T, Shan C, Ivaska A, Niu L (2010) Simultaneous determination of ascorbic acid, dopamine and uric acid with chitosan-graphene modified electrode. Electroanalysis 22:2001–2008. doi:10.1002/elan.201000094
35. Silva R, Lima AWO, Serrano SHP (2008) Simultaneous voltammetric detection of ascorbic acid, dopamine and uric acid using a pyrolytic graphite electrode modified into dopamine solution. Anal Chim Acta 612:89–98. doi:10.1016/j.aca.2008.02.017
36. Zhang Y, Pan Y, Su S, Zhang L, Li S, Shao M (2007) A novel functionalized single-wall carbon nanotube modified electrode and its application in determination of dopamine and uric acid in the presence of high concentrations of ascorbic acid. Electroanalysis 16:1695–1701. doi:10.1002/elan.200703901